Dalton Transactions

RSC Publishing

PAPER

View Article Online
View Journal | View Issue

Cite this: *Dalton Trans.*, 2013, **42**, 16102

Cathodic photocurrent generation from zinc-substituted cytochrome b_{562} assemblies immobilized on an apocytochrome b_{562}-modified gold electrode

Akira Onoda,* Yasuaki Kakikura and Takashi Hayashi*

Received 3rd June 2013,
Accepted 16th August 2013

DOI: 10.1039/c3dt51469b

www.rsc.org/dalton

Hierarchical assemblies of the noteworthy photoactive cytochrome b_{562} reconstituted with zinc protoporphyrin IX covalently linked with the protein surface were constructed on a gold electrode modified with an apoprotein of cytochrome b_{562}. The integrated photoactive hemoproteins were characterized by electrochemical impedance and quartz crystal microbalance analyses. The protein-immobilized electrode exhibits enhanced photocurrent generation relative to the one having a Zn-substituted hemoprotein monolayer.

Introduction

Creation of an electron-transfer interface between a redox-active protein and electrode is a key technological step toward further development of biosensors and photoelectric conversion biodevices.[1] To achieve an efficient electrochemical communication using a protein, many methodologies have been developed including protein immobilization which is mediated by noncovalent interactions, such as an electrostatic interaction with self-assembled monolayers (SAMs) on electrodes,[2] an affinity interaction with tag peptides[3] and a specific protein–cofactor interaction.[4] A further strategy to enhance the electrochemical communication is the accumulation of proteins on the electrode. The immobilization of proteins as multilayers has been reported using electrostatic interaction,[5] hydrophobic interaction,[6] interaction with polyelectrolytes,[7] and protein–nanoparticle interaction.[8]

Among the redox-active proteins, hemoproteins seem to be promising components for the construction of functional protein-immobilized electrodes due to their remarkable functions, such as electron transfer, catalysis, and sensing. Hemoprotein-immobilized electrodes have thus become of wide interest to evaluate their electrochemical behaviors[9] and/or generate a functional system, such as a biocatalyst,[10] a biosensor,[11] and a biofuel cell.[12]

We previously described the preparation of linear hemoprotein self-assemblies *via* a specific heme–heme pocket interaction, in which a heme moiety is externally attached to the surface of the H63C single mutant of cytochrome b_{562} (CYT)[13] or the A125C single mutant of myoglobin.[14] The supramolecular self-assembling systems of proteins[15] also allowed us to immobilize these assemblies on an electrode surface. We thus recently reported the construction of assemblies of photoactive hemoproteins connected with the photosensitizing cofactor, zinc protoporphyrin IX (ZnPP) derivatives,[2a,16] on a gold electrode and their enhanced electrochemical communication relative to a monolayer of the zinc-substituted protein.[17] The relationship between the function and the protein-assembly orientation on the electrode surface will be important. In this paper, we thus demonstrate the construction of assemblies of photoactive hemoproteins connected with ZnPP, in which each protein immobilized in an opposite orientation to the electrode, to investigate the effect of orientation (Scheme 1). The characterization and the photoelectrochemical behaviors of the photoactive hemoprotein assemblies are described.

Results and discussion

To anchor the protein oligomers on the gold electrode *via* the ZnPP–heme pocket interaction, a linker between a gold electrode and an apoprotein of the H63C mutant (apoCYT) was first prepared as follows: One of the terminal amino groups of 1,12-diaminododecane was protected with *t*-Boc and then the free amino group was converted to a maleimide moiety. After the deprotection of *t*-Boc, the obtained 1-(12-aminododecyl)-1*H*-pyrrole-2,5-dione precursor was then coupled with 3,3′-dithiobis(propionic acid) to yield linker **1**. The gold electrode was immersed in a mixed solution of mercaptopropionic acid (100 mM) and **1** (20 mM) to form the self-assembled monolayer (SAM) (Scheme 1b). The maleimide-modified electrode was immersed in the protein solution of apoCYT, and

Department of Applied Chemistry, Graduate School of Engineering, Osaka University, Suita, Osaka 565-0871, Japan. E-mail: onoda@chem.eng.osaka-u.ac.jp, thayashi@chem.eng.osaka-u.ac.jp; Fax: +81-6-6879-7930; Tel: +81-6-6879-7928

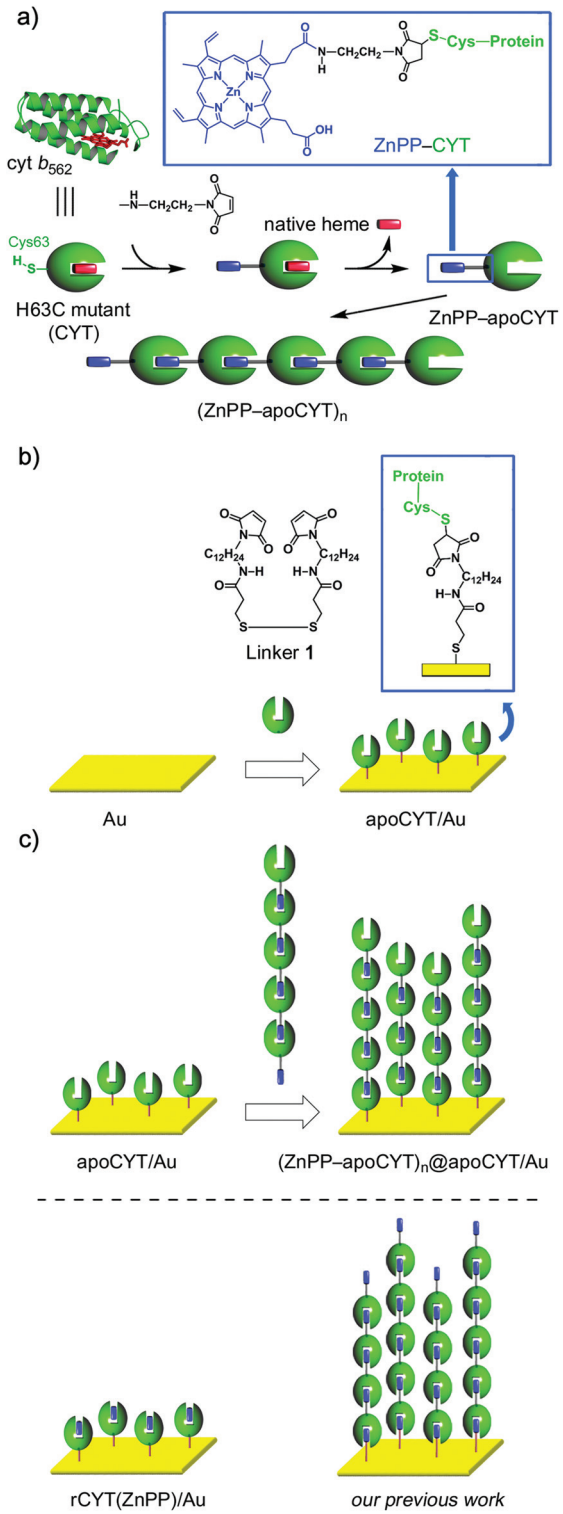

Scheme 1 (a) Supramolecular Zn-substituted cyt b_{562} assemblies.[18] Native heme (in red), ZnPP (in blue), and protein matrices (in green). (b) Preparation of an apoCYT-modified gold electrode. (c) Immobilization of the Zn-substituted cyt b_{562} assemblies on the apoCYT-modified electrode.

the unbound proteins in the solution were thoroughly washed away to provide an apoCYT-modified gold electrode (apoCYT/Au). The electrochemical impedance spectroscopy (EIS) indicates that the proteins are immobilized by a covalent linkage between the Cys residue of apoCYT and the maleimide on SAM (*vide infra*).

Next, according to our previous report, we prepared the photoactive protein oligomer, (ZnPP–apoCYT)$_n$, as shown in Scheme 1a.[17b] Coupling of the apoprotein on the gold electrode and noncovalent immobilization of (ZnPP–apoCYT)$_n$ were evaluated by the EIS measurement, which provides a sensitive detection of protein binding derived from the resistance changes at the electrode–solution interface. The measurements in Fig. 1 were performed in a buffered solution containing 5 mM $K_4[Fe(CN)_6]/K_3[Fe(CN)_6]$. The charge-transfer resistance R_{CT} for the maleimide-modified gold electrode was *ca.* 0.5×10^4 Ω, whereas an increased R_{CT} value (1.3×10^4 Ω) was observed after ZnPP-reconstituted CYT (rCYT(ZnPP)) was immobilized on the maleimide-modified electrode *via* the maleimide–Cys covalent linkage (rCYT(ZnPP)/Au). Furthermore, much larger resistance values, 2.5×10^4 Ω, were obtained when (ZnPP–apoCYT)$_n$ was immobilized on apoCYT/Au, indicating the construction of the integrated assemblies of the Zn-substituted CYT on the gold surface *via* noncovalent ZnPP–heme pocket interaction ((ZnPP–apoCYT)$_n$@apoCYT/Au).

To evaluate the degree of interprotein assemblies on the (ZnPP–apoCYT)$_n$@apoCYT/Au electrode, QCM measurements were conducted (Fig. 2). Upon the addition of zinc-substituted wild type cytochrome b_{562} (rCYT$_{WT}$(ZnPP)) without cysteine residue on the surface to the maleimide-modified electrode, only a slight frequency decrease was observed. In contrast, upon the addition of rCYT(ZnPP) with Cys, the frequency of the maleimide-immobilized QCM decreased by *ca.* 180 Hz.

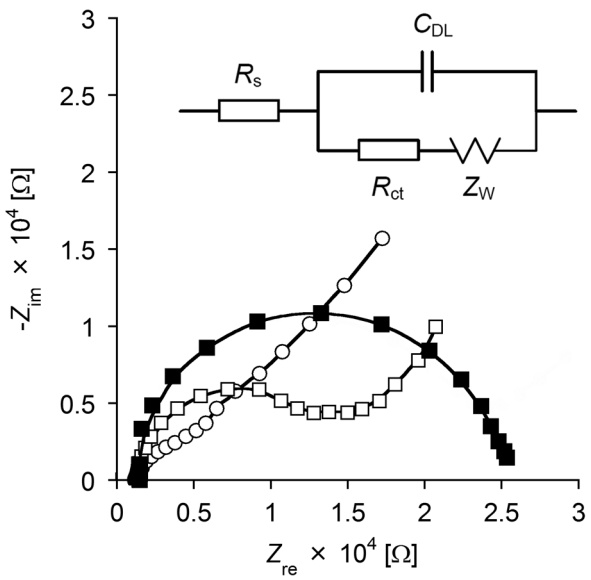

Fig. 1 Alternative-current impedance spectra of (ZnPP–apoCYT)$_n$@apoCYT/Au (■), rCYT(ZnPP)/Au (□), and maleimide-modified gold electrode (○) obtained in a 100 mM MOPS (pH 7.0) buffer containing 2.5 mM $K_3[Fe(CN)_6]$ and 2.5 mM $K_4[Fe(CN)_6]$. Fitted data are shown as solid lines. The biased potential was +0.10 V (*vs.* Ag|AgCl). The frequency was from 100 kHz to 0.01 Hz and the amplitude was 10.0 mV. The inset shows the equivalent circuit applied to the data fitting.

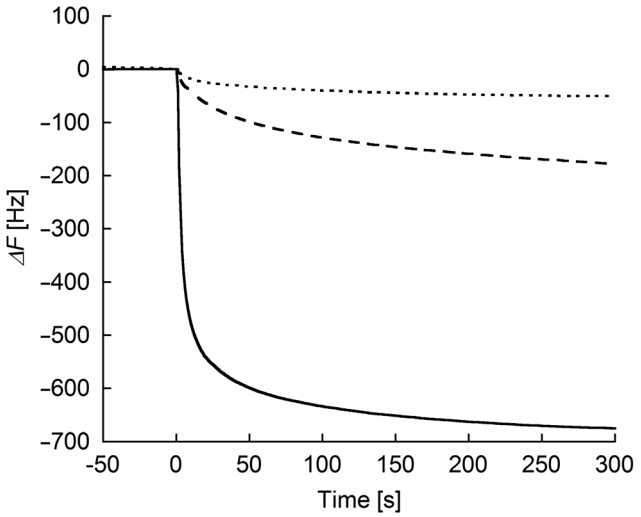

Fig. 2 Frequency changes in response to the addition of the proteins: $rCYT_{wt}$(ZnPP) (dotted line) and rCYT(ZnPP) (dashed line) to the maleimide-modified Au electrode, respectively, and $(ZnPP–apoCYT)_n$ (solid line) to the apoCYT/Au electrode. Samples were added into 500 μL of a buffered solution (100 mM KPi (pH 7.0)) in the QCM cell at 25 °C (final concentration of the sample was 4 μM).

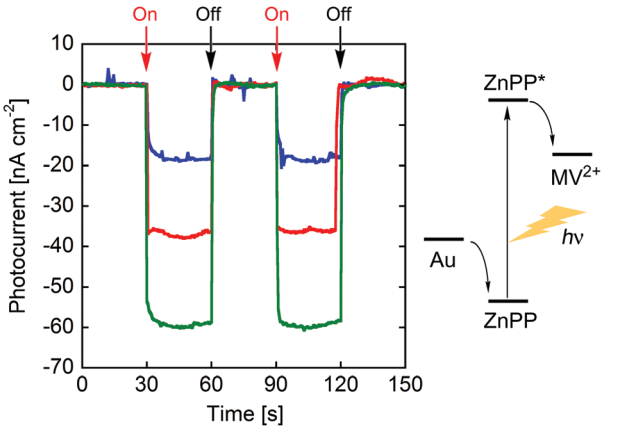

Fig. 3 Photocurrent response patterns of $(ZnPP–apoCYT)_n$@apoCYT/Au (in red), rCYT(ZnPP)/Au (in blue), and our previously reported hemoprotein assembly (in green)[17b] during on/off cycles of white light. The bias potential was −200 mV (*vs.* Ag|AgCl).

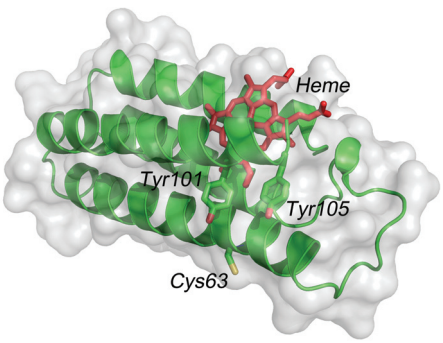

Fig. 4 The structure of cytb_{562} showing Tyr101 and Tyr105 residues between heme and Cys63.

This value is almost saturated upon the addition of excess rCYT(ZnPP), showing that the the rCYT(ZnPP) protein occupies the electrode surface *via* the covalent linkage. Furthermore, a significant frequency decrease upon the addition of $(ZnPP–apoCYT)_n$ (700 Hz) was observed, supporting the accumulation of ZnPP–apoCYT units on the electrode. Such a prominent frequency decrease was not observed when $(ZnPP–apoCYT)_n$ was added to the bare gold electrode. The average number (n) of the oligomer formation within the assemblies was estimated to be 3.8. The limited number of the assembly may stem from the non-specific interaction between the cofactors and the surface of the proteins, which were immobilized in a tightly packed fashion on the electrode surface.

Photocurrent measurements of $(ZnPP–apoCYT)_n$@apoCYT/Au employed as a working electrode were carried out to investigate the properties of the hierarchical protein assemblies containing the photosensitizer. Fig. 3 shows photocurrent response patterns of the prepared electrodes during on/off cycles of white light in the presence of methylviologen (MV^{2+}) as an electron acceptor. We observed the clear rise and fall of the cathodic current under the bias potential of −200 mV (*vs.* Ag|AgCl). When the electrode covalently immobilized with Zn-substituted CYT *via* Cys63 was irradiated with monochromatic light at 420 nm (0.043 mW), we observed a photocurrent response of 18 nA cm^{-2}, which was slightly increased relative to that found in the monomer-immobilized *via* ZnPP in our previous report (13 nA cm^{-2}). This suggests that the two Tyr residues which position between the heme pocket and Cys63 would be possibly involved in the electron transfer pathway from the electrode to ZnPP (Fig. 4). In addition, the photocurrents of $(ZnPP–apoCYT)_n$@apoCYT/Au were almost doubled (38 nA cm^{-2}), indicating that more densely layered assembly of the zinc-substituted proteins on the electrode surface enhances the photocurrent generation. Although the four layers of the protein including three layers of the photosensitizing moieties were assembled on average, the photocurrents increased only twice. This suggests that the proteins more distant from the electrode surface would be less efficient to generate photocurrents. We also found that our previously reported Zn-substituted cytochrome b_{562}, in which the zinc cofactor is located directly on the electrode, is more effective (60 nA cm^{-2}) than the assembly here in photocurrent generation (Fig. 3). Hence a smaller assembly (3.8 units) was formed relative to the previously reported system (7.0 units).

Conclusions

In conclusion, Zn-substituted hemoprotein assemblies *via* a specific noncovalent ZnPP–heme pocket interaction were constructed on the apocytochrome b_{562}-immobilized electrode, which was characterized by EIS and QCM measurements. The present work demonstrates that the fabricated supramolecular assemblies of a photoactive electron transfer protein in the

orientation opposite to our previously reported system also generate cathodic photocurrents. Efforts to expand the attractive features of hemoprotein assemblies with a controlled orientation by this strategy to photoelectric conversion are now in progress.

Experimental

Instruments

^{1}H NMR spectra (400 MHz) were recorded using a Bruker DPX400 NMR spectrometer, and chemical shifts are reported in ppm relative to the residual solvent resonances. ESI-TOF MS analyses were performed using a Bruker Daltonics micrOTOF. UV-Vis spectra were taken using a Shimadzu UV-3150 or UV-2550 spectrophotometer equipped with a thermostated cell holder. The pH values were monitored using an F-52 Horiba pH meter. Quartz-crystal microbalance (QCM) measurements were performed using AFFINIX $Q_N\mu$ (Initium, Japan). Electrochemical measurements were made with a potentiostat (CompactStat, Ivium Technologies) using a platinum wire as a counter electrode and standard Ag|AgCl as a reference electrode. The electrolyte was 100 mM MOPS buffer (pH 7.0) containing 5 mM $K_4[Fe(CN)_6]/K_3[Fe(CN)_6]$.

Materials

Zinc protoporphyrin IX with maleimide at the propionate side chain,[17b] mono-*N*-Boc protected 1,12-dodecane diamine[13c] and 3,3′-dithiobis(propionic acid) were prepared according to a previous report.[19] Other reagents and chemicals were purchased and used as received. The H63C mutant of cytochrome b_{562} (CYT) was expressed in *E. coli* and purified as previously reported.[13c,20] Zinc protoporphyrin IX was obtained by a conventional procedure. Apo forms of proteins (apoCYT and $apoCYT_{wt}$), the reconstituted proteins with zinc protoporphyrin IX (rCYT(ZnPP) and $rCYT_{wt}$(ZnPP)), and the photoactive protein oligomer (ZnPP–apoCYT)$_n$ were prepared according to the methods of previous reports with modification.[16b,17b]

Synthesis

1-(12-Aminododecyl)-1*H*-pyrrole-2,5-dione trifluoroacetate. To a suspension of maleic anhydride (93.0 mg, 0.954 mmol) in 80 mL of benzene, a solution of mono-*N*-Boc protected 1,12-dodecane diamine (260 mg, 0.867 mmol) in 40 mL of benzene was added. The resulting mixture was stirred at room temperature for 1 h, and $ZnBr_2$ (215 mg, 0.954 mmol) and hexamethyl disilazane (209 mg, 1.30 mmol) in 20 mL of benzene were then added. The resulting suspension was refluxed for 2 h. After cooling to room temperature, the reaction mixture was poured into 20 mL of 0.5 M HCl_{aq}. The organic layer was separated and the aqueous portion was extracted twice with 150 mL portions of CH_2Cl_2. The combined organic layers were washed with saturated aqueous $NaHCO_3$ (150 mL × 2), brine (150 mL × 1), and dried over Na_2SO_4. The solution was then filtered, and the filtrate was dried under vacuum to yield the crude product, *N*-Boc protected 1-(12-aminododecyl)-1*H*-pyrrole-2,5-dione, as a white solid. To a solution of *N*-Boc protected 1-(12-aminododecyl)-1*H*-pyrrole-2,5-dione in 10 mL of CH_2Cl_2 was added 3 mL of trifluoroacetic acid. The solution was stirred for 4 h at room temperature. After the solvent was evaporated, the residue was dissolved in a minimal amount of MeOH. By adding isopropyl ether to the solution, a white solid was precipitated to give trifluoroacetate salt of 1-(12-aminododecyl)-1*H*-pyrrole-2,5-dione (161 mg, 0.575 mmol, 67%). ^{1}H NMR (400 MHz, $CDCl_3$) δ 7.84 (br, 2H), 6.71 (s, 2H), 3.52 (t, J = 7.2, 2H), 2.93 (t, J = 7.2, 2H), 1.64–1.26 (m, 20H); ESI-TOF MS (positive mode) m/z calcd for $C_{16}H_{28}N_2O_2$ $[M + H]^+$ 281.22, found 281.24.

Synthesis of 1. Both 1-(12-aminododecyl)-1*H*-pyrrole-2,5-dione trifluoroacetate (120 mg, 0.428 mmol) and 3,3′-dithiobis(propionic acid) (40.0 mg, 0.190 mmol) were mixed in dry CH_2Cl_2, and then *N*-(3-dimethylaminopropyl)-*N*′-ethyl carbodiimide hydrochloride (363 mg, 1.9 mmol) was added under a N_2 atmosphere at 0 °C. The mixture was stirred for 6 h at room temperature and then filtered. After the removal of the solvent, the resulting mixture was extracted with CH_2Cl_2 and washed with brine (50 mL × 3). The organic layer was dried over anhydrous Na_2SO_4. The product was purified by column chromatography (SiO_2, CH_2Cl_2–MeOH = 10/1 → 5/1(v/v)) to yield **2** as a white solid (157 mg, 0.214 mmol, 50%). ^{1}H NMR (400 MHz, $CDCl_3$) δ 6.71 (s, 4H), 6.35 (br, 2H) 3.53 (t, J = 7.2, 4H), 3.37 (t, J = 7.2, 4H), 1.60–1.27 (m, 48H); ESI-TOF MS (negative mode) m/z calcd for $C_{38}H_{62}N_4O_6S_2$ $[M + Cl]^-$ 769.38, found 769.27.

Preparation of modified gold electrodes

A gold-coated quartz slide (AuroSheet(111), Tanaka Kikinzoku Kogyo K.K., Japan) with (111) surface (>80%) was used as an electrode. An electrochemically cleaned gold electrode was modified by soaking in 300 μL of a DMSO solution of mercaptopropionic acid (100 mM) and **1** (20 mM) to form a self-assembled monolayer. After incubation for 6 h at room temperature, the electrode was thoroughly rinsed with water and then immersed in a 100 μM protein solution (apoCYT, rCYT(ZnPP)) in 200 μL of 10 mM Tris-HCl buffer (pH 7.0) to give the electrode modified with each protein.

Quartz-crystal microbalance (QCM) measurements

QCM measurements were performed using a cell equipped with a 27 MHz QCM plate oscillating at the fundamental frequency. The maleimide- or apoCYT-immobilized QCM cell was filled with 500 μL of a buffered solution (10 mM KPi, pH 7.0), and the time course frequency changes were observed on the addition of the protein solution (4 μM (ZnPP–apoCYT)$_n$, rCYT(ZnPP), or $rCYT_{wt}$ (ZnPP)).

Photocurrent measurements

Photocurrent measurements were performed in a typical three-electrode configuration connected to a potentiostat as reported previously.[17b] A 50 mM Tris-HCl (pH 7.5) containing methylviologen (1 mM) was used. The maximum current with clear photoresponses was obtained under the bias potential of −200 mV.

Acknowledgements

This work was supported by Grants-in-Aid for Scientific Research ((B), KAKENHI 17350085 and Innovative Areas "Coordination Programming", area 2107, KAKENHI 22108518, 24108726) from MEXT and the Japan Society for the Promotion of Science (JSPS). Y.K. acknowledges support from the Global COE Program of Osaka University and from JSPS. A.O. acknowledges support from the Frontier Research Base for Global Young Researchers, Osaka University, on the Program of MEXT, and from the Ogasawara Foundation. T.H. acknowledges support from the Asahi Grass Foundation.

Notes and references

1 (*a*) I. Willner and E. Katz, *Bioelectronics*, Wiley-VCH, Weinheim, 2005; (*b*) L. Fruk, C. H. Kuo, E. Torres and C. M. Niemeyer, *Angew. Chem., Int. Ed.*, 2009, **48**, 1550–1574; (*c*) L.-Y. Cheng, Y.-T. Long, H.-B. Kraatz and H. Tian, *Chem. Sci.*, 2011, **2**, 1515–1518; (*d*) N. Terasaki, N. Yamamoto, T. Hiraga, Y. Yamanoi, T. Yonezawa, H. Nishihara, T. Ohmori, M. Sakai, M. Fujii, A. Tohri, M. Iwai, Y. Inoue, S. Yoneyama, M. Minakata and I. Enami, *Angew. Chem., Int. Ed.*, 2009, **48**, 1585–1587; (*e*) M. Miyachi, Y. Yamanoi, Y. Shibata, H. Matsumoto, K. Nakazato, M. Konno, K. Ito, Y. Inoue and H. Nishihara, *Chem. Commun.*, 2010, **46**, 2557–2559.

2 (*a*) Y. Tokita, J. Shimura, H. Nakajima, Y. Goto and Y. Watanabe, *J. Am. Chem. Soc.*, 2008, **130**, 5302–5310; (*b*) Y. Tokita, S. Yamada, W. Luo, Y. Goto, N. Bouley-Ford, H. Nakajima and Y. Watanabe, *Angew. Chem., Int. Ed.*, 2011, **50**, 11663–11666; (*c*) K. Nakano, T. Yoshitake, Y. Yamashita and E. F. Bowden, *Langmuir*, 2007, **23**, 6270–6275.

3 (*a*) C. Ley, D. Holtmann, K. M. Mangold and J. Schrader, *Colloids Surf., B*, 2011, **88**, 539–551; (*b*) N. Terasaki, M. Iwai, N. Yamamoto, T. Hiraga, S. Yamada and Y. Inoue, *Thin Solid Films*, 2008, **516**, 2553–2557.

4 (*a*) Y. Xiao, F. Patolsky, E. Katz, J. F. Hainfeld and I. Willner, *Science*, 2003, **299**, 1877–1881; (*b*) M. Zayats, E. Katz, R. Baron and I. Willner, *J. Am. Chem. Soc.*, 2005, **127**, 12400–12406; (*c*) A. Das and M. H. Hecht, *J. Inorg. Biochem.*, 2007, **101**, 1820–1826; (*d*) H. Zimmermann, A. Lindgren, W. Schuhmann and L. Gorton, *Chem.–Eur. J.*, 2000, **6**, 592–599; (*e*) L. H. Guo, G. McLendon, H. Razafitrimo and Y. L. Gao, *J. Mater. Chem.*, 1996, **6**, 369–374.

5 R. Dronov, D. G. Kurth, H. Möhwald, R. Spricigo, S. Leimkühler, U. Wollenberger, K. V. Rajagopalan, F. W. Scheller and F. Lisdat, *J. Am. Chem. Soc.*, 2008, **130**, 1122–1123.

6 P. N. Ciesielski, C. J. Faulkner, M. T. Irwin, J. M. Gregory, N. H. Tolk, D. E. Cliffel and G. K. Jennings, *Adv. Funct. Mater.*, 2010, **20**, 4048–4054.

7 F. Lisdat, R. Dronov, H. Möhwald, F. W. Scheller and D. G. Kurth, *Chem. Commun.*, 2009, **46**, 274–283.

8 L. Frolov, O. Wilner, C. Carmeli and I. Carmeli, *Adv. Mater.*, 2008, **20**, 263–266.

9 (*a*) K. Kobayashi, M. Shimizu, T. Nagamune, H. Sasabe, Y. Fang and W. Knoll, *Bull. Chem. Soc. Jpn.*, 2002, **75**, 1707–1713; (*b*) D. H. Murgida and P. Hildebrandt, *Phys. Chem. Chem. Phys.*, 2005, **7**, 3773–3784; (*c*) A. E. F. Nassar, W. S. Willis and J. F. Rusling, *Anal. Chem.*, 1995, **67**, 2388–2392; (*d*) I. Taniguchi, K. Watanabe, M. Tominaga and F. M. Hawkridge, *J. Electroanal. Chem.*, 1992, **333**, 331–338; (*e*) J. Xu, F. Shang, J. H. T. Luong, K. M. Razeeb and J. D. Glennon, *Biosens. Bioelectron.*, 2010, **25**, 1313–1318.

10 (*a*) E. E. Ferapontova, *Electroanalysis*, 2004, **16**, 1101–1112; (*b*) F. W. Scheller, U. Wollenberger, C. Lei, W. Jin, B. Ge, C. Lehmann, F. Lisdat and V. Fridman, *Rev. Mol. Biotech.*, 2002, **82**, 411–424.

11 (*a*) N. Bistolas, U. Wollenberger, C. Jung and F. W. Scheller, *Biosens. Bioelectron.*, 2005, **20**, 2408–2423; (*b*) Y. Wu and S. Hu, *Microchim. Acta*, 2007, **159**, 1–17.

12 (*a*) G. X. Ma, T. H. Lu and Y. Y. Xia, *Bioelectrochemistry*, 2007, **71**, 180–185; (*b*) A. Ramanavicius and A. Ramanaviciene, *Fuel Cells*, 2009, **9**, 25–36.

13 (*a*) H. Kitagishi, Y. Kakikura, H. Yamaguchi, K. Oohora, A. Harada and T. Hayashi, *Angew. Chem., Int. Ed.*, 2009, **48**, 1271–1274; (*b*) H. Kitagishi, K. Oohora and T. Hayashi, *Biopolymers*, 2009, **91**, 194–200; (*c*) H. Kitagishi, K. Oohora, H. Yamaguchi, H. Sato, T. Matsuo, A. Harada and T. Hayashi, *J. Am. Chem. Soc.*, 2007, **129**, 10326–10327; (*d*) A. Onoda, Y. Ueya, T. Sakamoto, T. Uematsu and T. Hayashi, *Chem. Commun.*, 2010, **46**, 9107–9109; (*e*) A. Onoda, A. Takahashi, K. Oohora, Y. Onuma and T. Hayashi, *Chem. Biodiversity.*, 2012, **9**, 1684–1692; (*f*) K. Oohora, A. Onoda and T. Hayashi, *Chem. Commun.*, 2012, **48**, 11714–11726.

14 (*a*) K. Oohora, A. Onoda, H. Kitagishi, H. Yamaguchi, A. Harada and T. Hayashi, *Chem. Sci.*, 2011, **2**, 1033–1308; (*b*) K. Oohora, S. Burazerovic, A. Onoda, Y. M. Wilson, T. R. Ward and T. Hayashi, *Angew. Chem., Int. Ed.*, 2012, **51**, 3818–3821.

15 (*a*) M. M. C. Bastings, T. F. A. de Greef, J. L. J. van Dongen, M. Merkx and E. W. Meijer, *Chem. Sci.*, 2011, **1**, 79–88; (*b*) J. C. Carlson, S. S. Jena, M. Flenniken, T. F. Chou, R. A. Siegel and C. R. Wagner, *J. Am. Chem. Soc.*, 2006, **128**, 7630–7638; (*c*) S. Burazerovic, J. Gradinaru, J. Pierron and T. R. Ward, *Angew. Chem., Int. Ed.*, 2007, **46**, 5510–5514; (*d*) D. A. Uhlenheuer, K. Petkau and L. Brunsveld, *Chem. Soc. Rev.*, 2010, **39**, 2817–2826; (*e*) H. D. Nguyen, D. T. Dang, J. L. J. van Dongen and L. Brunsveld, *Angew. Chem., Int. Ed.*, 2010, **49**, 895–898.

16 (*a*) E. Topoglidis, C. J. Campbell, E. Palomares and J. R. Durrant, *Chem. Commun.*, 2002, 1518–1519; (*b*) S. Takeda, N. Kamiya and T. Nagamune, *Biotechnol. Lett.*, 2004, **26**, 121–125; (*c*) T. Matsuo, A. Asano, T. Ando, Y. Hisaeda and T. Hayashi, *Chem. Commun.*, 2008, 3684–3686; (*d*) Y. Hitomi, T. Hayashi, K. Wada, T. Mizutani, Y. Hisaeda and H. Ogoshi, *Angew. Chem., Int. Ed.*, 2001, **40**, 1098–1101.

17 (*a*) Y. Kakikura, A. Onoda, E. Kubo, H. Kitagishi, T. Uematsu, S. Kuwabata and T. Hayashi, *J. Inorg. Organomet. Polym. Mater.*, 2013, **23**, 172–179; (*b*) A. Onoda, Y. Kakikura, T. Uematsu, S. Kuwabata and T. Hayashi, *Angew. Chem., Int. Ed.*, 2012, **51**, 2628–2631.
18 ZnPP contains regioisomers with respect to the substitution position at the two heme-propionate side chains of protoporphyrin IX.
19 M. C. Daniel and D. Astruc, *Chem. Rev.*, 2004, **104**, 293–346.
20 A. Onoda, T. Himiyama, K. Ohkubo, S. Fukuzumi and T. Hayashi, *Chem. Commun.*, 2012, **48**, 8054–8056.